THE JOURNAL OF BIOLOGICAL CHEMISTRY VOL. 287, NO. 6, pp. 4211–4221, February 3, 2012
Published in the U.S.A.

Hydrogen Sulfide Is an Endogenous Potentiator of T Cell Activation*[S]

Received for publication, September 27, 2011, and in revised form, December 5, 2011 Published, JBC Papers in Press, December 13, 2011, DOI 10.1074/jbc.M111.307819

Thomas W. Miller[‡], Evelyn A. Wang[‡], Serge Gould[‡], Erica V. Stein[‡], Sukhbir Kaur[‡], Langston Lim[§], Shoba Amarnath[¶], Daniel H. Fowler[¶], and David D. Roberts[‡1]

From the [‡]Laboratory of Pathology, Center for Cancer Research, [§]Laboratory of Experimental Carcinogenesis, Center for Cancer Research, and [¶]Experimental Transplantation and Immunology Branch, NCI, National Institutes of Health, Bethesda, Maryland 20892

Background: T cells encounter H_2S in physiological and pathophysiological settings with unknown consequences.
Results: Exogenous and endogenous H_2S enhances T cell activation.
Conclusion: T cell activation depends on H_2S signaling.
Significance: H_2S can act as an autocrine or paracrine T cell activator and suggests a mechanistic link to inflammatory bowel disease progression.

H_2S is an endogenous signaling molecule that may act via protein sulfhydrylation to regulate various physiological functions. H_2S is also a byproduct of dietary sulfate metabolism by gut bacteria. Inflammatory bowel diseases such as ulcerative colitis are associated with an increase in the colonization of the intestine by sulfate reducing bacteria along with an increase in H_2S production. Consistent with its increased production, H_2S is implicated as a mediator of ulcerative colitis both in its genesis or maintenance. As T cells are well established mediators of inflammatory bowel disease, we investigated the effect of H_2S exposure on T cell activation. Using primary mouse T lymphocytes (CD3+), OT-II CD4+ T cells, and the human Jurkat T cell line, we show that physiological levels of H_2S potentiate TCR-induced activation. Nanomolar levels of H_2S (50–500 nM) enhance T cell activation assessed by CD69 expression, interleukin-2 expression, and CD25 levels. Exposure of T cells to H_2S dose-dependently enhances TCR-stimulated proliferation with a maximum at 300 nM (30% increase, $p < 0.01$). Furthermore, activation increases the capacity of T cells to make H_2S via increased expression of cystathionine γ-lyase and cystathionine β-synthase. Disrupting this response by silencing these H_2S producing enzymes impairs T cell activation, and proliferation and can be rescued by the addition of 300 nM H_2S. Thus, H_2S represents a novel autocrine immunomodulatory molecule in T cells.

H_2S is emerging as an important member of the gasotransmitter family. At toxic environmental concentrations (>200 ppm), H_2S inhibits mitochondrial cytochrome *c* oxidase (1). Lower nontoxic concentrations have potential physiological functions in neuromodulation (Ref. 2; for review, see Ref. 3), metabolic hibernation (4, 5), protection from ischemia/reperfusion injury (6–10), oxygen sensing (11), vasodilatation (12, 13), and promotion of angiogenesis (14). In common with nitric oxide, H_2S is also implicated as both a pro- (15–18) and anti-inflammatory (18–21) molecule in innate immune cells. Although the role of H_2S signaling has been characterized in many other tissues and systems, it is unclear what role it plays in the regulation of the adaptive immune system.

H_2S is produced from dietary sulfate metabolism in the lumen of the large intestine by anaerobic sulfate-reducing bacteria (22). Clinical studies indicate that inflammatory bowel diseases such as ulcerative colitis are associated with an increase in the colonization of the intestine by sulfate-reducing bacteria along with an increase in the levels of H_2S produced (23–27).

T cells also make an attractive target to study H_2S signaling due to the lack of trans-sulfuration enzymes cystathionine γ-lyase (CSE)[2] and cystathionine β-synthase (CBS) in naive cells (28, 29) and the extensive literature characterizing the sensitivity of T cells to extracellular thiol redox status (30–32). In contrast to naïve cells, activated T cells may be capable of making H_2S (33), although the proliferation of a cytotoxic $CD8^+$ subset was inhibited by what we now consider supraphysiological doses of H_2S (34). Therefore, we examine here whether T cell activation is affected by physiological concentrations of exogenous H_2S and whether endogenous H_2S production is required for T cell activation.

MATERIALS AND METHODS

Cells and Reagents—H_2S refers to any of its various protonation states ($H_2S \rightarrow HS^- + H^+ \rightarrow S^{2-} + H^+$) with HS^- being the predominant form at physiological pH ($pK_a = 6.8$). Na_2S and NaHS are the corresponding sodium salts of these anionic forms of H_2S and are thus considered H_2S donors at physiological pH and are used as sources of H_2S for this study. GYY4137 is also used as a slow-releasing H_2S donor as characterized in Li

* This work was supported, in whole or in part, by the National Institutes of Health Intramural Research Program of the National Cancer Institute, Center for Cancer Research (Grant 1ZIA SC 009174).
[S] This article contains supplemental Figs. S1 and S2.
[1] To whom correspondence should be addressed: NIH, Bldg. 10 Rm. 2A33, 10 Center Dr. MSC1500, Bethesda, MD 20892-1500. E-mail: droberts@helix.nih.gov.

[2] The abbreviations used are: CSE, cystathionine γ-lyase; CBS, cystathionine β-synthase; MTOC, microtubule organizing complex; TCR, T cell receptor; MTS, 3-(4,5-dimethylthiazol-2-yl)-5-(3-carboxymethoxyphenyl)-2-(4-sulfophenyl)-2H-tetrazolium; SQR, sulfide quinone oxidoreductase; EYFP, enhanced YFP.

et al. (35) and Lee *et al.* (36). C57Bl/6 and OT-II mice were anesthetized and sacrificed by cervical dislocation, and their spleens were harvested for T cell culture. OT-II mice and OVA_{1-47} were kind gifts of the laboratory of Dr. Richard Morgan (NCI, NIH). The spleens were gently ruptured in a 40-μm cell strainer (BD Biosciences) placed over a 50-ml Falcon tube using the back end of a 6-cc syringe plunger. The cells were rinsed-through with basal RPMI (0.1% BSA) and centrifuged at 200 $\times$ *g* for 5 min. CD3+ T cells were purified by using a pan T cell isolation kit II and MACS MS columns (Miltenyi Biotec) without prior red-cell lysis according to the manufacturer's protocol. The cells were resuspended in 10 ml of RPMI containing 10% FBS, glutamine, and penicillin/streptomycin and plated in a flask for 30 min at 37 °C and 5% CO_2. Care and handling of animals was in accordance with the Animal Care and Use Committees of the National Cancer Institute (Protocol LP-012).

Wild-type Jurkat T cells (E6.1, ATCC), enhanced GFP-actin, and EYFP-tubulin expressing clones (a kind gift of Dr. Lawrence Samelson, NIH (37)) were maintained at 2–5 $\times$ 10^5 cells per ml in RPMI supplemented with glutamine, penicillin/streptomycin, and 10% FBS. Cells were maintained in culture for a maximum of 4 weeks. For cell activation studies, Jurkat cells were resuspended in basal medium (RPMI, glutamine, penicillin/streptomycin, and 0.1% BSA).

Unless specified otherwise, all chemicals were purchased from Sigma. GYY4137 was purchased from Cayman Chemicals (Ann Arbor, MI). For T cell activation, wells of either 6- or 96-well plates were coated overnight with a mixture of anti-CD3 and anti-CD28 antibodies (mouse cells, clones 17A2 and 37.51, respectively, BD Biosciences; Jurkat cells, OKT3 and CD28.2, functional grade, eBioscience) at 2 and 5 μg/ml, respectively, in PBS without cations. The following day wells were washed twice with PBS to remove unbound antibody, and cells were added in growth medium for stimulation.

The concentrations of H_2S used for this study are derived from the EC_{50} concentrations of H_2S (from NaHS or Na_2S) used for stimulation of T cell proliferation (see Fig. 3). Also, the steady state concentration of H_2S will depend on how much is added exogenously or made endogenously and the rate of its degradation. The degradation of H_2S both enzymatically and nonenzymatically depends largely on O_2 concentration (38). Minimizing the O_2 levels maximizes available H_2S. Due to this, we conducted the experiments at 1% O_2 and 94% N_2 using a hypoxic chamber (MIC-101, Billups-Rothenberg, Inc., Del Mar, CA) unless stated otherwise.

Flow Cytometry—T cells were washed with PBS supplemented with 0.1% BSA and 0.01% azide (FACS buffer) and stained using anti-CD69-FITC (BD Biosciences) or anti-CD25 (BD Biosciences) and analyzed with a FACS Caliber and CellQuest software (BD Biosciences).

Cell Adhesion Assay—To monitor cell adhesion we used an ACEA real time label-free cell monitoring system (Xcelligence, Roche Applied Science) (39). 50 μl of basal media was allowed to incubate for 15 min in each well of an 8-well RT-CES plate at 37 °C, 5% CO_2. An additional 50 μl containing 25,000 Jurkat cells and the specified treatments were added to the wells, and the cell index was measured at 30-s intervals. All data are normalized to 15 min after cell addition, when all cells have settled to the bottom of the well.

TABLE 1
Primer sequences for RT-PCR
h, human; m, mouse; HPRT, hypoxanthine-guanine phosphoribosyltransferase.

Gene	Forward	Reverse
mHPRT	gttaagcagtacagccccaaa	agggcatatccaacaacaaactt
mCD69	acgctcttgttctgaagatgctgc	tccaatgttccagttcacca
mIL-2	ttggacctctgcggcatgttc	caaatgtgttgtcagagccct
mCBS	agaagtgccctggctgtaaa	caggactgtcgggatgaagt
mCSE	tgctgccaccattacgatta	gatgccaccctcctgaagta
mSQR	agtagctgcccagtctggaa	taccagtgggcacgaggtat
hHPRT	attgtaatgaccagtcaacag	gcattgttttgccagtgtcaa
hCD69	ctggtcacccatggaagtgc	acattccatgctgctgacct
hIL-2	cctgccacaatgtacaggatgca	ggtgcactgtttgtgacaagtgc
hCBS	ggcctgaagtgtgagctctt	ttggggatttcgttcttcag
hCSE	ctaagtcaaagcgggtcagc	cccacagaggtttgtccact

Fluorescence Microscopy—Antigen-presenting cells often vary in the distribution of major histocompatibility complexes, making the use of an antibody-coated surface advantageous in these experiments as it provides a simpler and more homogenous stimulus necessary for quantifying cytoskeletal changes (37). The glass surface also allows for a single orientation of activated cells and a high degree of cell polarization. The microtubule organizing complex (MTOC) of Jurkat cells that are maximally activated by the antibody-coated surface should be at the center of the cell contact point (*x,y* plane) and directly above the contact surface (*x,z* plane) (40). Likewise, previous studies have indicated that TCR-specific antibody-coated microspheres can serve as artificial antigen-presenting cells by providing a focal stimulus capable of inducing MTOC reorientation to the immunological synapse (41). Both are used to assess cytoskeletal changes in this study.

8-Chambered Lab-tek coverslips (Nunc) were coated with either 0.01% w/v poly-L-lysine solution (Sigma) or anti-CD3/anti-CD28 antibodies (1 and 5 μg/ml) in PBS overnight at 4 °C and then washed with PBS. EYFP-tubulin- or enhanced GFP-actin-expressing Jurkat cells (50,000 cells) in basal RPMI medium were added to the wells and allowed to incubate at 37 °C, 5% CO_2 with specified treatments before imaging on the confocal microscope. Confocal images were acquired on a Zeiss LSM 510 NLO confocal system (Carl Zeiss, Thornwood, NJ) with a 63$\times$ Plan-Apochromat 1.4 NA oil immersion objective. Z-stacked images were acquired at 512 $\times$ 512 pixels per frame using an 8-bit pixel depth for each channel and line averaging set to 4 collected sequentially in a multi-track, 3 channel mode.

Gene Expression Studies—In 6-well plates, 1–3 $\times$ 10^6 cells for each condition were maintained in 1 or 20% O_2 for the specified amount of time. The cells were harvested, and mRNA was extracted using TRIzol (Invitrogen) according to the manufacturer's protocol. cDNA was synthesized from 1–5 μg of mRNA using superscript first-strand RT-PCR reagents (Invitrogen) according to the manufacturer's protocol. Quantitative real-time-PCR was then performed using the SYBR Green kit (Thermo) on the following gene/primer sets: hypoxanthine phosphoribosyltransferase, CD69, IL-2, CSE, CBS, SQR (sequences Table 1). Hypoxanthine phosphoribosyltransferase was used as the internal control for expression based on previous reports of its superior stability over other commonly used control genes (42). Results were calculated based

on the ΔCt method and normalized to hypoxanthine phosphoribosyltransferase.

T Cell Proliferation—Cells were seeded at 100,000 cells per well in 96-well plates uncoated or precoated with anti-CD3/CD28 as specified above and treated as indicated. Proliferation was assessed using cell titer-96 MTS reagent (Promega) after 72 h of growth according to the manufacturer's protocol. The MTS signal for the cells on day 0 was subtracted from the signal after 72 h to quantify net proliferation. Proliferation was also assessed by CFSE dilution (Invitrogen) in murine CD3+ cells using flow cytometry. CFSE-based proliferation was analyzed using Flow Jo software. Cells were maintained in 1 or 20% O_2 as indicated.

IL-2 Transcription Factor Luciferase Assays—The reporter plasmid for the IL-2 promoter elements CD28RE-Luc, NFAT-Luc, STAT5-Luc, CRE-Luc, NFκB-Luc, and AP1-Luc were kind gifts of Dr. Kevin Gardner (43) constructed in PGL3-basic luciferase plasmids (Promega). Jurkat T cells (2×10^6) were co-transfected with 5 μg of each reporter plasmid and 1 μg of the *Renilla* luciferase construct using an Amaxa nucleofector system (program X-001). After transfection, the cells were cultured in RPMI containing 10% FBS, glutamine, and penicillin/streptomycin overnight followed by stimulation in antibody-coated 96-well plates for the indicated amount of time (determined by time-course for maximum signal). Cells were lysed by adding 20 μl of passive lysis buffer to 100 μl of cells for 5 min after triturating. The dual luciferase reporter assay system (Promega) was used for the quantification of reporter gene expression. Luciferase activities were determined using a Turner Biosystems 20/20N luminometer. Transcription factor-driven firefly luciferase activity was normalized by dividing firefly luciferase units by the units corresponding to *Renilla* luciferase activity.

Intracellular cGMP Assay—Jurkat cells were assayed at 5×10^5 cells per condition in 0.5 ml of basal media (RPMI, glutamine, penicillin/streptomycin, 0.01% BSA). The cells were incubated for 4 h with the indicated concentrations of NaHS and diethylenetriamine/NONOate at 37 °C. The cells were then lysed, and total intracellular cGMP levels were measured via an immunoassay using a cGMP kit (GE/Amersham Biosciences) according to the manufacturer's instructions. cGMP levels were normalized to control non-diethylenetriamine/NONOate-treated samples.

siRNA Knockdown Experiments—siRNAs were synthesized using the Silencer siRNA Construction kit (AP Biosystems). Three different siRNAs were made to target each gene (CBS and CSE) based on primers selected from the Ambion siRNA target finder web application. Each siRNA transfection represented in the text is an equal mixture of each of the following three individual siRNAs targeting unique exons for maximum potency (sequences in Table 2).

Mouse T cells were harvested as above, and $CD3^+$ T cells were purified by using a pan T cell isolation kit II and MACS MS columns (Miltenyi Biotec) without prior red-cell lysis according to the manufacturer's protocol. Purified T cells were then transfected with 30 pmol of siRNA cocktails using a mouse T cell nucleofection kit and an Amaxa nucleofector (program X-01) according to the manufacturer's protocol. Jurkat cells were maintained in antibiotic-free RPMI growth medium and transfected using nucleofection kit V and program X-01 according to the manufacturer's protocol. After transfection, the cells were cultured in RPMI containing 10% FBS, glutamine, and penicillin/streptomycin 16 h followed by stimulation in antibody-coated 96-well plates for 72 h with specified analyses.

TABLE 2
Sequences for siRNA synthesis

Human siRNAs; CBS
Exon 4
Sense strand siRNA, GGGGUCCCCAGAGGAUAAGtt
Antisense strand siRNA, CUUAUCCUCUGGGGACCCCtt
Exon 7
Sense strand siRNA, GAUGAGCUCCGAGAAGGUGtt
Antisense strand siRNA, CACCUUCUCGGAGCUCAUCtt
Exon 16
Sense strand siRNA, AGUCAUCUACAAGCAGUUCtt
Antisense strand siRNA, GAACUGCUUGUAGAUGACUtt
Mouse siRNAs
CSE
Exon 1
Sense strand siRNA, GAGCCUGAGCAAUGGAAUUtt
Antisense strand siRNA, AAUUCCAUUGCUCAGGCUCtt
Exon 2
Sense strand siRNA, CAAGGAAUUGCUUGGAAAAtt
Antisense strand siRNA, UUUUCCAAGCAAUUCCUUGtt
Exon 4
Sense strand siRNA, AACCAAAUUGCUAGAGGCAtt
Antisense strand siRNA, UGCCUCUAGCAAUUUGGUUtt
CBS
Exon 14
Sense strand siRNA, GUCUGCAAAGUCCUCUACAtt
Antisense strand siRNA, UGUAGAGGACUUUGCAGACtt
Exon 10
Sense strand siRNA, GUGGUUCAAGAGCAACGAUtt
Antisense strand siRNA, AUCGUUGCUCUUGAACCACtt
Exon 9
Sense strand siRNA, ACAGCCUAUGAGGUGGAAGtt
Antisense strand siRNA, CUUCCACCUCAUAGGCUGUtt

RESULTS

H_2S Enhances TCR-stimulated T Cell Activation—We first assessed the effect of physiological (nM) H_2S concentrations on T cell activation. CD69 expression is one of the earliest events following TCR-mediated T cell activation (44). Using quantitative real-time-PCR to assess CD69 mRNA expression, anti-CD3/CD28 stimulation of freshly isolated mouse T cells led to a time-dependent increase in CD69 expression (Fig. 1*A*). CD69 expression was significantly ($p < 0.05$) increased at 4 and 10 h post-stimulation in the presence of 300 nM H_2S. Mouse T cell CD69 expression was also dose-dependently increased at 6 h post-stimulation in the presence of H_2S (50, 500 nM) by 30 and 100%, respectively (Fig. 1*B*). Other markers of T cell activation were also enhanced in the presence of 300 nM H_2S such as IL-2 and CD25 mRNA expression (Fig. 1, *C* and *D*). Human Jurkat T-lymphoma cells serve as a continuous cell line that is widely used to study T cell activation. CD69 and IL-2 induction were similarly enhanced in Jurkat cells activated by anti-CD3 and CD28 antibodies (Fig. 1, *E* and *F*). Consistent with increases in CD69 mRNA, CD69 protein expression was enhanced by polyclonal activation (Fig. 1*G*) and was dose-dependently enhanced by H_2S in activated Jurkat cells (Fig. 1*H*). CD69 expression was enhanced by 27% in the presence of 100 nM H_2S and 33% in the presence of 50 μM of the H_2S donor molecule GYY4137 corresponding to a steady state H_2S concentration of 200 nM (Fig. 1*I*).

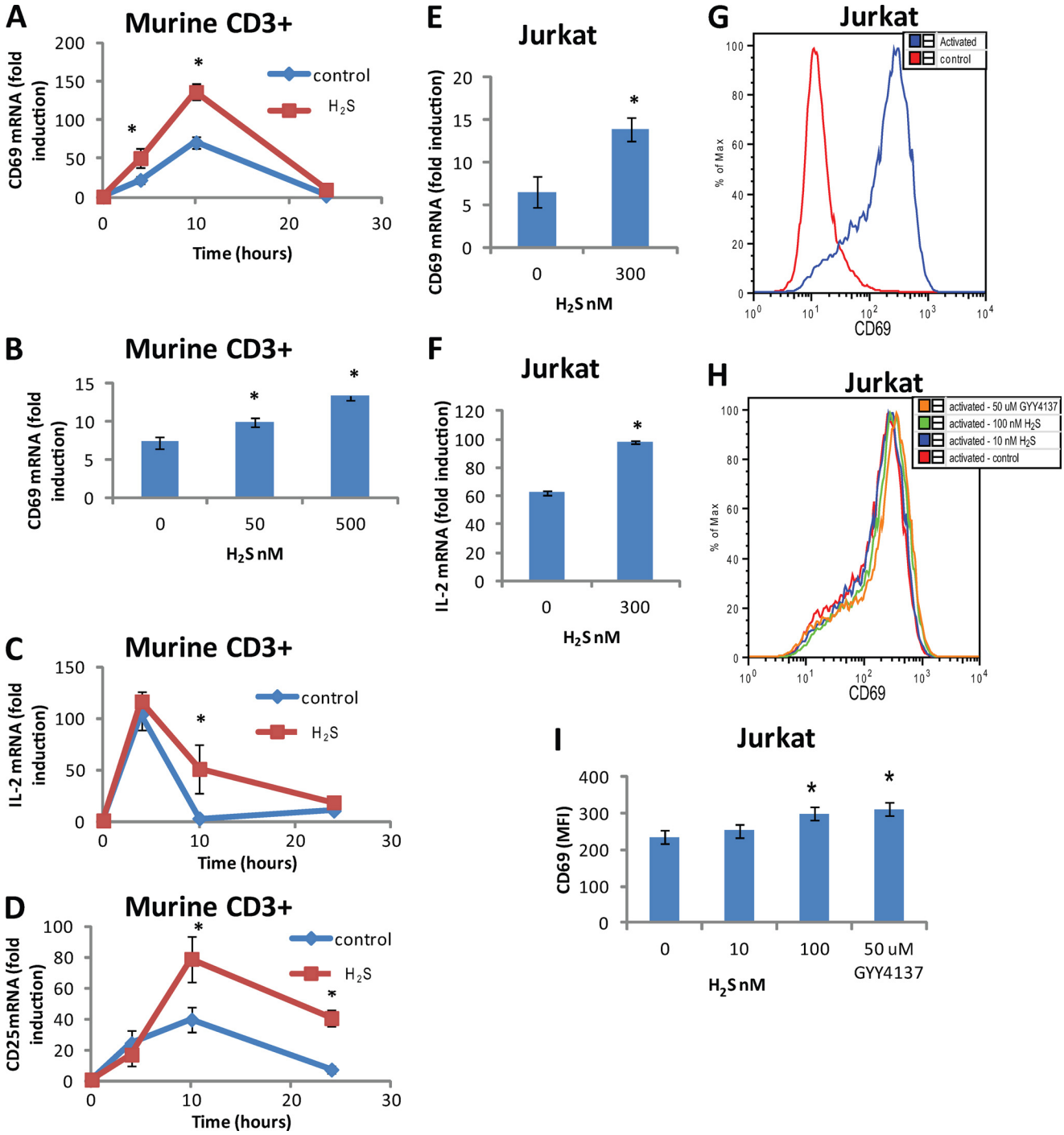

FIGURE 1. **H_2S enhances TCR-stimulated T cell activation.** *A*, *C*, and *D*, murine CD3+ (3×10^6 cells) were activated with plate-bound anti-CD3/CD28 antibodies in the presence of 300 nM Na_2S or vehicle in 1% O_2, and gene expression of CD69 (*A*), IL-2 (*C*), and CD25 (*D*) was examined by RT-PCR at 4, 10, and 24 h. *B*, CD69 gene expression was examined in murine CD3+ cells at 4 h after activation with plate-bound anti-CD3/CD28 antibodies in 1% O_2 by RT-PCR in the presence of 50 and 500 nM Na_2S or vehicle. CD69 (*E*) and IL-2 (*F*) gene expression was examined in Jurkat cells (3×10^6 cells) at 4 h after activation with plate-bound anti-CD3/CD28 antibodies in 1% O_2 by RT-PCR in the presence of 300 nM Na_2S or vehicle. *G* and *H*, CD69 protein expression was examined in Jurkat cells 24 h after activation with plate-bound anti-CD3/CD28 antibodies in 1% O_2 by flow cytometry in the presence of 10 and 100 nM Na_2S or vehicle. *I*, shown is a graphic representation of mean fluorescence intensity data in *H*. Data are normalized to non-activated control for each treatment; $n = 3$, *error bars* indicate S.D. *, denotes $p < 0.05$.

In addition to polyclonal stimulation of T cell activation, we tested the ability of H_2S to enhance antigen-specific T cell activation. CD4+ T cells freshly isolated from OT-II mice were co-stimulated with 1 μg/ml OVA-2 peptide and 5 μg/ml anti-CD28 antibody with and without H_2S treatment (300 nM). H_2S significantly enhanced OVA-2 peptide stimulation of IL-2 expression at 6 and 24 h (Fig. 2*A*). In addition, 100 nM H_2S enhanced OVA-2 stimulation of CD25 protein levels by 30% (Fig. 2*B*).

H_2S Enhances Activation-dependent Cytoskeletal Dynamics in T Cells—T cell activation induces cytoskeletal rearrangements necessary for full activation and polarization toward an antigen-presenting cell (45, 46). Activation-dependent

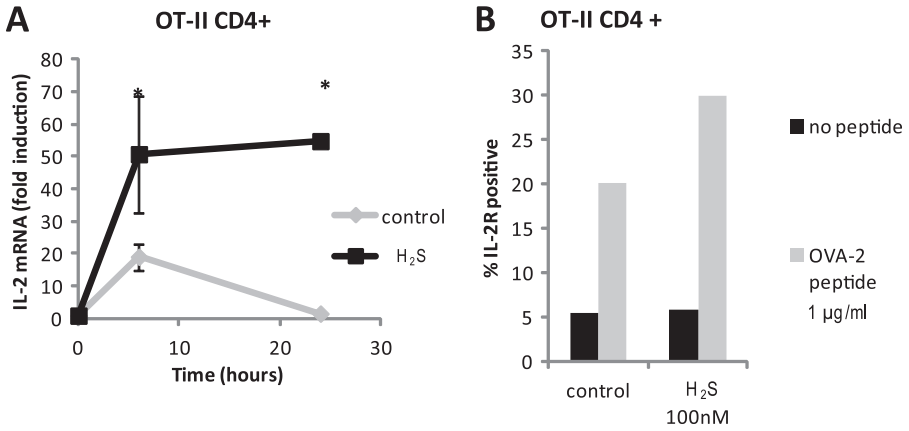

FIGURE 2. **H_2S enhances antigen-specific T cell activation.** Murine CD4+ OT-II T cells (3×10^6 cells) were activated with a combination of 1 μg/ml OVA2 peptide and 5 μg/ml anti-CD28 antibody in the presence of 300 nM Na_2S or vehicle in 1% O_2, and gene expression of IL-2 was examined by RT-PCR at 4, 10, and 24 h (*A*). Data are normalized to non-activated control for each treatment; $n = 3$, *error bars* indicate S.D. *, denotes $p < 0.05$. *B*, IL-2 receptor (CD25) was measured in the presence or absence of 100 nM Na_2S by flow cytometry. Data are representative of $n = 2$.

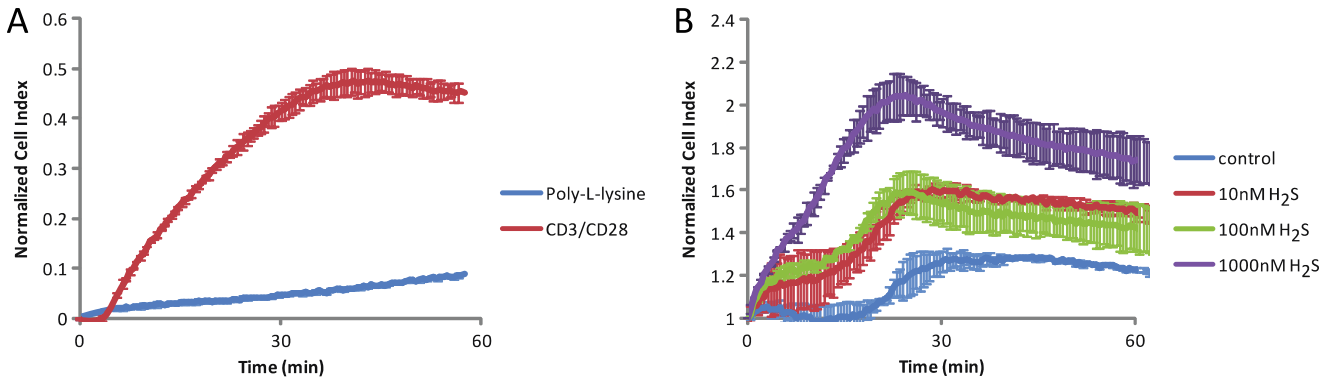

FIGURE 3. **H_2S enhances T cell attachment to the TCR-stimulating surface.** Cell attachment was assessed at 20% O_2 using an ACEA real time cell analyzer. Jurkat cells (25,000) were added to either poly-L-lysine or anti-CD3/CD28 coated wells without treatment (*A*) or to anti-CD3/CD28-coated wells with Na_2S treatment (*B*), and the cell index was monitored at 30-s intervals.

spreading and attachment of T cells depends on cytoskeletal dynamics in the MTOC and actin cytoskeleton. The key cytoskeletal elements actin and β-tubulin were identified as direct sulfhydrylation targets of endogenous H_2S produced in mouse liver (47). H_2S sulfhydrylation of actin *in vitro* resulted in enhanced polymerization. However, this was only observed at supraphysiological (100–200 μM) levels of H_2S. We addressed the function of these targets at physiological H_2S concentrations. Jurkat T cells were plated on a surface coated with anti-CD3/CD28, and adhesion was quantified by measuring impedance at this interface expressed as a normalized cell index. As expected, cells attached more firmly on anti-CD3/CD28-coated surfaces as compared with poly-L-lysine-coated surfaces (Fig. 3*A*). This signal was dose-dependently enhanced in the presence of 10 nM to 1 μM Na_2S (Fig. 3*B*). Thus, physiological doses of H_2S enhance T cell interaction with a TCR activating surface.

MTOC translocation was assessed in Jurkat cells stably transfected with EYFP-α-tubulin and stimulated using anti-CD3/CD28-coated microspheres to induce an immunological synapse. Previous studies have indicated that TCR-specific antibody-coated microspheres can serve as artificial antigen-presenting cells by providing a focal stimulus capable of inducing MTOC reorientation to the immunological synapse (41). Microsphere activation alone resulted in MTOC translocation directly adjacent to the microsphere in 34 ± 2% of the cells (Fig. 4*A*). Co-treatment with 300 nM Na_2S significantly enhanced this translocation (53 ± 5 *versus* 34 ± 2, $p < 0.05$, Fig. 4, *A* and *B*).

The enhancement of MTOC translocation by H_2S was further analyzed by imaging the interaction of EYFP-α-tubulin-expressing Jurkat cells with control or anti-CD3/CD28 coated glass surfaces. Antigen-presenting cells often vary in the distribution of major histocompatibility complexes, making use of an antibody-coated surface advantageous in these experiments, as it provides a simpler and more homogenous stimulus necessary for quantifying cytoskeletal changes (37). The glass surface also allows for a single orientation of activated cells and a high degree of cell polarization. The MTOC of Jurkat cells that are maximally activated by the antibody-coated surface should be at the center of the cell contact point (*x*,*y* plane) and directly above the contact surface (*x*,*z* plane) (40). Although MTOCs had mostly random orientation on the control surfaces, greater than 60% were centrally oriented in the *x*,*y* plane on the activating surface (Fig. 4*C*). Na_2S treatment significantly increased this positioning to 90% (Fig. 4*D*). Interestingly, in the three-dimensional rendering of the *x*,*z* plane, the MTOC was properly located at the activating surface for both Na_2S, treated and untreated, but the tubulin cytoskeleton of the Na_2S-

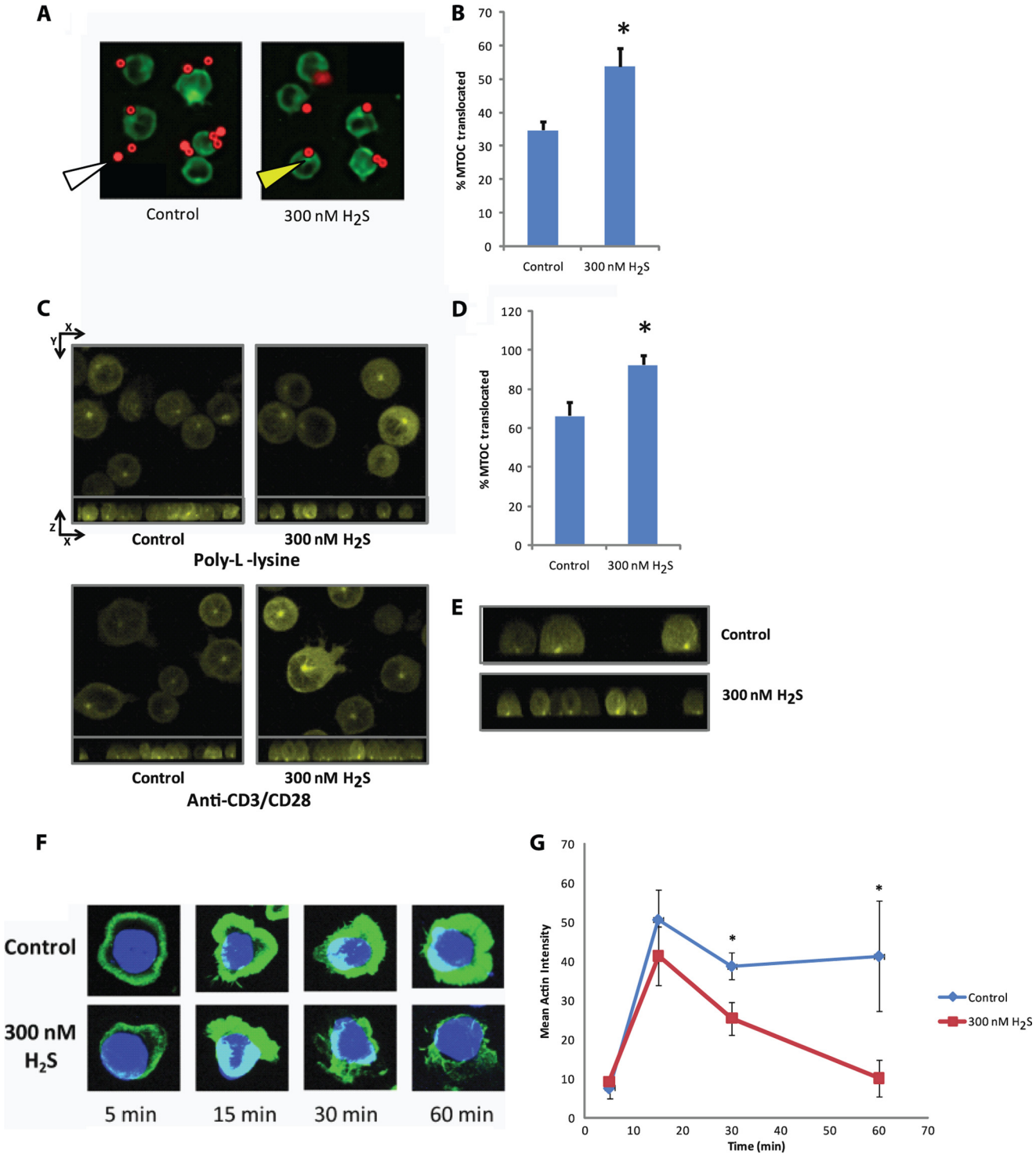

FIGURE 4. **H_2S targets the cytoskeleton in activated T cells.** *A*, anti-CD3/CD28-coated magnetic beads (*red*) were incubated with EYFP-α-tubulin expressing Jurkat cells (*pseudo-colored green*) in the presence or absence of 300 nM Na_2S for 15 min at 20% O_2. *Yellow arrow* = MTOC; *white arrow* = microsphere. *B*, MTOC orientation to the anti-CD3/CD28-coated magnetic beads was quantified as % translocated. $n = 50$ cells for each condition. *, denotes $p < 0.05$. *C*, EYFP-α-tubulin expressing Jurkat cells (25,000) were added to either poly-L-lysine or anti-CD3/CD28-coated glass coverslips with or without 300 nM Na_2S and incubated for 45 min before confocal images of z-stacks were taken. At the *top of each panel* is the composite image of the *x,y* plane and directly under is the *x,z* plane. *D*, MTOC orientation to the center of the immunological synapse created at the glass surface was quantified as % translocated. $n > 25$ cells for each condition. * denotes $p < 0.05$. *E*, shown are images from the *x,z* plane anti-CD3/CD28-coated portion of *D* cropped to a single cell depth. *F*, the actin cytoskeleton (*green*) of fixed Jurkat cells was stained with phalloidin after stimulation with anti-CD3/CD28 in the presence or absence of 300 nM Na_2S for the denoted times and imaged using confocal microscopy. Images are maximum projection composites of Z-stacks. *G*, quantified intensity of actin staining at each time point is shown.

treated cells was much more uniformly elongated than untreated cells (Fig. 4*E*). Thus, exogenous H_2S enhances MTOC dynamics in activated T cells.

Likewise, the response of the actin cytoskeleton to anti-CD3/CD28 activation was notably altered by treatment with 300 nM Na_2S (Fig. 4*F*). Control and Na_2S-treated cells form a distinct

actin collar within the first 5 min after plating on anti-CD3/CD28 surfaces. This actin collar significantly increased in intensity until 15 min (Fig. 4*G*). Subsequently, breakdown in the actin collar occurs in the Na_2S-treated cells after 15 min, whereas the control cells maintain this collar. These data are consistent with the Jurkat cell adhesion data in Fig. 3*B* showing greater dynamics in the presence of H_2S. Dynamic regulation of the actin cytoskeleton at the immunological synapse enhances downstream signaling from the TCR (48), which can be disrupted by actin polymerization targeting drugs such as cytochalasin D (49, 50).

We also investigated several previously defined targets of H_2S in other systems, including K^+ATP channels, cGMP-dependent phosphodiesterases (51), and Akt (52) and found that these are not responsible for the effects of H_2S on T cell activation (supplemental Fig. 1).

H_2S Biosynthetic Capacity Is Increased with T Cell Activation—As a diffusible gasotransmitter, we considered whether H_2S could act as an autocrine and paracrine mediator of TCR-stimulated proliferation in a manner similar to IL-2. Expression of the two major H_2S biosynthetic genes, CBS and CSE was notably increased over that in resting T cells after activation, 150 and 250%, respectively (Fig. 5, *A* and *B*). Steady state levels of H_2S also depend on its rate of degradation via SQR, an O_2-dependent mitochondrial enzyme (53, 54). SQR was slightly decreased in activated *versus* resting T cells (Fig. 5*C*), implying that higher levels of H_2S are present in activated T cells. Consistent with this concept, uptake of the CBS and CSE substrate cysteine is dramatically increased upon T cell activation (55). Thus, the capacity of activated T cells to make H_2S is enhanced, implying that H_2S acts as an autocrine regulator of T cell activation.

Endogenous H_2S Regulates T Cell Activation—Unlike naïve T cells, Jurkat cells express CBS (28, 29). To address the role of endogenous H_2S produced by CBS on cell adhesion, Jurkat cells were transfected with CBS siRNA. The decreased expression of CBS mRNA (Fig. 6*A*) resulted in decreased adhesion, which could be partially rescued by the addition of exogenous H_2S (300 nM Na_2S, Fig. 6*B*). Gene expression levels were reduced by greater than 50% compared with scrambled control RNA in Jurkat cells treated with CBS-specific siRNA. siRNA knockdown of endogenous H_2S-producing capacity via CBS significantly impaired both CD69 and IL-2 expression in TCR-activated Jurkat cells (Fig. 6, *C* and *D*). Because CD69 and IL-2 protein levels correlate well with mRNA levels (56), our data indicate that physiological levels of exogenous and endogenous H_2S control critical aspects of T cell activation and signaling.

To further address the role of endogenously produced H_2S in activated T cells, we assessed the activation-dependent proliferation of purified mouse CD3+ T cells in the presence of H_2S. TCR stimulation of T cells induces proliferation and supports their *in vitro* polyclonal expansion in part via autocrine and paracrine IL-2 signaling (57, 58). Proliferation of TCR-stimulated mouse spleen-derived T cells was enhanced in a biphasic manner by 30–300 nM NaHS (Fig. 6*E*) as assessed using an MTS proliferation assay. These results are supported by a CFSE staining experiment showing a similar increase in proliferation index of CD8 cells treated with 300

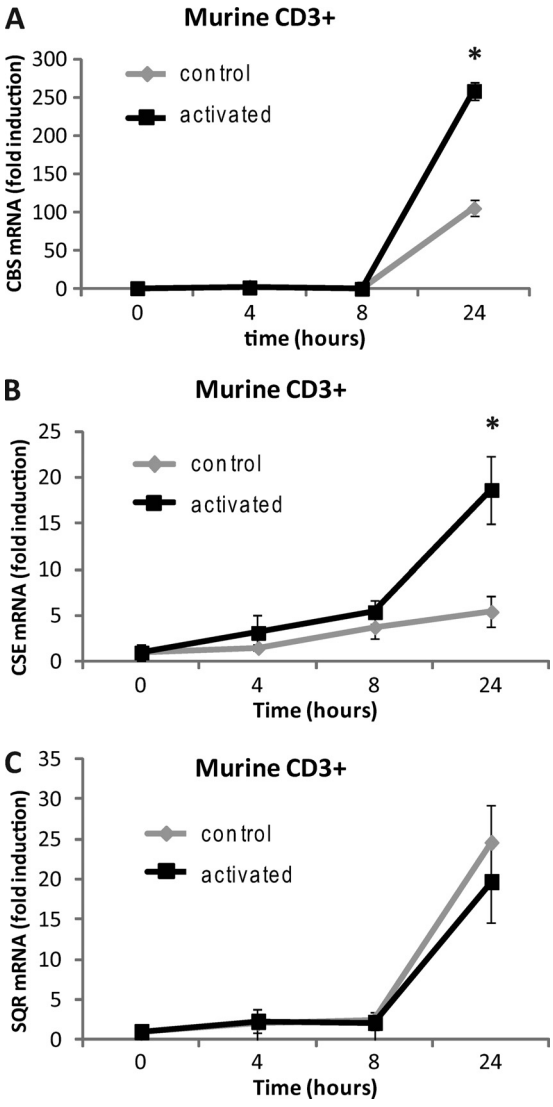

FIGURE 5. **T cell activation increases the capacity for H_2S production.** Purified mouse CD3+ T cells were activated with plate-bound anti-CD3/CD28 antibodies, and gene expression of CBS (*A*), CSE (*B*), and SQR (*C*) were examined in 1% O_2 by RT-PCR at 24 h. Data are normalized to non-activated control for each treatment; $n = 3$, *error bars* indicate S.D. * denotes $p < 0.05$.

nM H_2S (supplemental Fig. 2). In a 20% O_2 atmosphere, maximal enhancement of proliferation was 30% at 300 nM NaHS. We compared the effects of H_2S on proliferation at 1% O_2 because enzymatic and nonenzymatic degradation of H_2S is O_2-dependent (38). We then assessed proliferation due to endogenous H_2S via siRNA knockdown of CBS and CSE. Targeting either CBS or CSE with siRNAs decreased the proliferation of TCR-activated T cells by about 20% (Fig. 6*F*). However, targeting both enzymes inhibited TCR-driven proliferation as compared with scrambled siRNA control by nearly 40%. In all cases proliferation was rescued by adding back 300 nM NaHS.

DISCUSSION

These data demonstrate physiological functions of endogenous and exogenous H_2S in T cell activation. TCR-dependent T cell activation and IL-2 expression are enhanced by H_2S, and activation in turn increases expression of H_2S biosynthetic

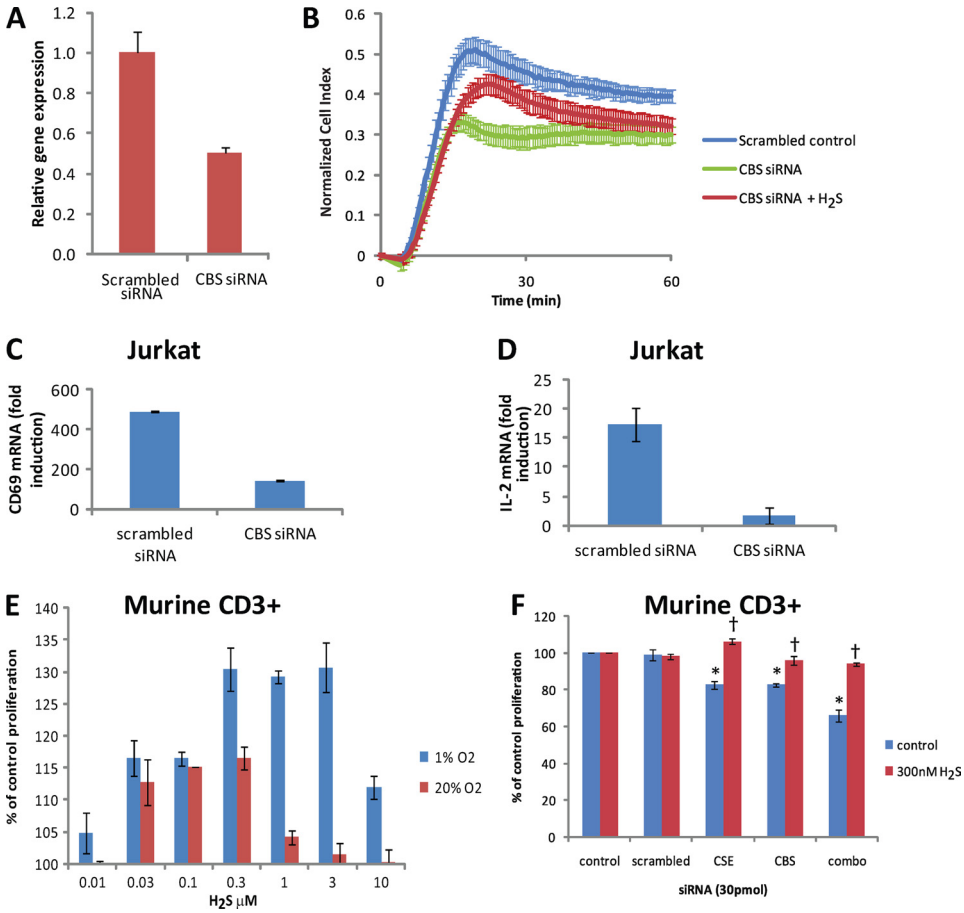

FIGURE 6. **T cells depend on endogenous H_2S for proliferation.** *A*, cell attachment was assessed using an ACEA real time cell analyzer. Jurkat cells were transfected with either nonspecific scrambled or CBS-specific siRNA. CBS gene expression was monitored after 24 h. *B*, siRNA-transfected Jurkat cells were added to anti-CD3/CD28-coated wells 24 h after transfection with or without 300 nM Na_2S. *Error bars* represent S.D. for $n = 2$. Graphs are representative of multiple experiments. *C* and *D*, CD69 and IL-2 gene expression were examined after nonspecific scrambled or CBS-specific siRNA transfection of Jurkat T cells after a 4-h activation by plate-bound anti-CD3/CD28 antibodies. Data are normalized to non-activated control for each treatment; $n = 3$, *error bars* indicate S.D. *E*, proliferation was assessed in mouse CD3+ T cells in the presence of Na_2S (0.01–10 μM) at both 1 and 20% O_2 levels and after transfection with pooled siRNAs specific for CBS and CSE or a nonspecific scrambled control (*F*). Cells were activated with plate-bound anti-CD3/CD28 antibodies in the presence of Na_2S or vehicle, and proliferation was assessed in a 1% O_2 atmosphere via an MTS assay at 72 h post-activation. Data represent net proliferation relative to day 0 and are normalized to non-activated controls for each treatment; $n = 3$, *error bars* indicate S.D. *, denotes $p < 0.05$ compared with scrambled; †, denotes $p < 0.05$ compared with no H_2S control.

enzymes without altering expression of the major H_2S degradative enzyme SQR (Fig. 7). This function of H_2S was validated for general and antigen-specific T cell activation of murine T cells and for the human Jurkat T cell line. The effects of H_2S are mediated at least in part by enhanced microtubule and actin cytoskeletal dynamics that, along with work by the Snyder laboratory, suggest that the cytoskeleton is a direct and sensitive physiological target of H_2S (47).

Despite having several clearly defined signaling roles, the levels of endogenously produced H_2S that mediate these functions are in dispute, and the most recent measurement in tissue homogenates is 15 nM (59). This lower estimate calls into question several proposed physiological targets of H_2S that require micromolar H_2S levels to modulate their activities (60–62). Mustafa *et al.* (47) identified actin and β-tubulin, key elements of the cytoskeleton, as direct targets of endogenous H_2S produced in murine liver. H_2S sulfhydrylation of actin resulted in enhanced polymerization and a visible change in the actin cytoskeleton; however, this was only observed *in vitro* at supraphysiological levels of exogenously added H_2S (100–200 μM).

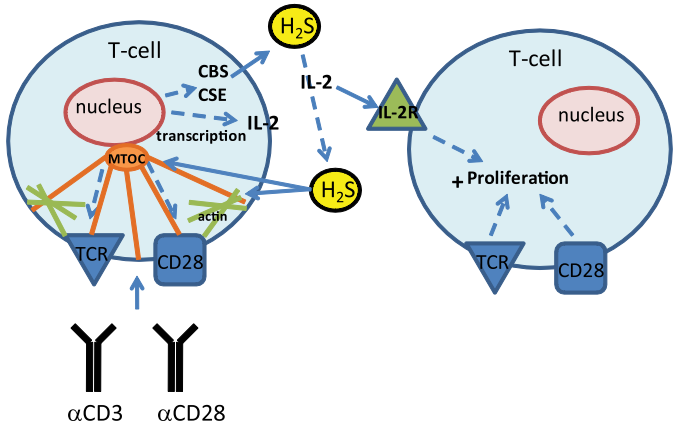

FIGURE 7. **A schematic of the proposed H_2S signaling in T cells.** Exogenous H_2S enhances TCR-stimulated T cell activation and IL-2 expression. The target of H_2S may be the actin and tubulin cytoskeleton, as their dynamics are enhanced in the presence of H_2S. T cell activation also depends on endogenous H_2S production by CBS and CSE, which are increased by T cell activation. The production of H_2S by activated T cells may act as an autocrine or paracrine enhancer of T cell activation. *IL-2R*, IL-2 receptor.

We sought to examine the effect of H_2S on the cytoskeleton at physiological levels in T cells. During antigen-dependent T cell activation, cytoskeletal rearrangement is essential for full activation and polarization of the T cell toward the antigen-presenting target cell (45, 46). The actin cytoskeleton polymerizes to provide a physical scaffold for the assembly of T cell receptor proteins as well as for the associated supramolecular activation complex. The tubulin cytoskeleton reorganizes to radiate vectorially outward from the center of the supramolecular activation complex to its MTOC. Compounds that disrupt microtubule or actin polymerization, such as taxol, colchicine, or cytochalasin D, inhibit antigen-dependent and IL-2-driven T cell proliferation (49, 50). T cells also make an attractive target due to the lack of transsulfuration enzymes (CSE and CBS) in naive cells (28, 29) and the extensive literature characterizing the sensitivity of T cells to extracellular thiol redox status (30–32).

Although our studies present the cytoskeleton as one possible target of H_2S-dependent T cell activation, the proliferation data are biphasic, suggesting that additional concentration-dependent H_2S targets exist. Also, the maximal effect was greater at low O_2, consistent with an O_2-mediated degradative mechanism. This confirms numerous other reports of a complex relationship between O_2 and H_2S in the cell. Because we did not observe a simple leftward shift in H_2S effect with a decrease in O_2, we suggest that there may not be a simple single ligand receptor relationship for H_2S signaling in these cells.

In contrast to naïve cells, activated T cells are capable of making H_2S. Peripheral blood lymphocytes were previously reported to produce H_2S, although this biosynthetic activity was not specifically attributable to T cells (33). Furthermore, H_2S inhibited proliferation of cytotoxic CD8+ T cells; however, this occurred at what we now consider to be a supraphysiological concentration of H_2S (34). In contrast, our data establish that proliferating T cells depend on their endogenous capacity to generate H_2S, and this capacity is enhanced by T cell activation. In addition to this autocrine role, H_2S may have a paracrine function in T cell activation. This idea is supported by the report of increased H_2S output from activated antigen presenting cells (63). Peripheral T cell activation and proliferation must be tightly controlled to prevent autoimmune destruction of cells and tissue. To achieve this, resting T cells are limited in their ability to take up basic amino acids such as cysteine (or cystine). T cells lack efficient transport of cystine and rely on a steady production by neighboring antigen-presenting cells to support their proliferation. Although not completely understood, the cysteine requirement of activated T cells is reportedly for making GSH and also participates in changing the extracellular thiol redox status to a more reducing environment, thus altering the activity of exofacial membrane-bound signaling proteins. We postulate that the additional cysteine demand could also satisfy the up-regulated H_2S synthesis necessary for full T cell proliferation. More recently, Garg *et al.* (64) reported that CBS protein levels are increased in T cells from BALBc mice activated by dendritic cells and an anti-CD3 antibody. Their results also indicate that the transsulfuration pathway is intact in naïve T cells as a source of cysteine to make glutathione, as cysteine and cystine uptake is limited. Consumption of cysteine for biosynthesis from the transsulfuration pathway would preclude the generation of H_2S from cysteine. We hypothesize that during T cell activation, when cysteine is no longer limited, that the transsulfuration enzymes CBS and CSE supply H_2S to support T cell activation and function while consuming cysteine.

This work could have important implications to the pathogenesis of inflammatory bowel disease. Inflammatory bowel disease is a chronic inflammatory disease caused by the generation and persistence of colitogenic CD4+ effector and memory T cells that react to antigens of commensal bacteria. H_2S is continually produced by luminal sulfate-reducing commensal bacteria in the colon and is normally detoxified by rhodanese in the surrounding mucosal cells to thiosulfate (65, 66). An increase in the steady state H_2S levels either from overproduction or reduced consumption is thought to play a role in the etiology of inflammatory bowel disease and related cancers (67). Our data provide a logical link between these reports in that the excess H_2S could contribute to unwanted T cell activation toward commensal H_2S-producing bacteria. Combined with the novel physiological signaling function for H_2S as a co-stimulator of T cell activation and proliferation, these findings establish H_2S as an endogenous and exogenous co-regulatory signal for T cells.

REFERENCES

1. Reiffenstein, R. J., Hulbert, W. C., and Roth, S. H. (1992) Toxicology of hydrogen sulfide. *Annu. Rev. Pharmacol. Toxicol.* **32,** 109–134
2. Abe, K., and Kimura, H. (1996) The possible role of hydrogen sulfide as an endogenous neuromodulator. *J. Neurosci.* **16,** 1066–1071
3. Tan, B. H., Wong, P. T., and Bian, J. S. (2010) Hydrogen sulfide. A novel signaling molecule in the central nervous system. *Neurochem. Int.* **56,** 3–10
4. Blackstone, E., Morrison, M., and Roth, M. B. (2005) H_2S induces a suspended animation-like state in mice. *Science* **308,** 518
5. Blackstone, E., and Roth, M. B. (2007) Suspended animation-like state protects mice from lethal hypoxia. *Shock* **27,** 370–372
6. Fu, Z., Liu, X., Geng, B., Fang, L., and Tang, C. (2008) Hydrogen sulfide protects rat lung from ischemia-reperfusion injury. *Life Sci.* **82,** 1196–1202
7. Jha, S., Calvert, J. W., Duranski, M. R., Ramachandran, A., and Lefer, D. J. (2008) Hydrogen sulfide attenuates hepatic ischemia-reperfusion injury. Role of antioxidant and antiapoptotic signaling. *Am. J. Physiol. Heart Circ. Physiol.* **295,** H801–H806
8. Tripatara, P., Patel, N. S., Collino, M., Gallicchio, M., Kieswich, J., Castiglia, S., Benetti, E., Stewart, K. N., Brown, P. A., Yaqoob, M. M., Fantozzi, R., and Thiemermann, C. (2008) Generation of endogenous hydrogen sulfide by cystathionine γ-lyase limits renal ischemia/reperfusion injury and dysfunction. *Lab. Invest.* **88,** 1038–1048
9. Elrod, J. W., Calvert, J. W., Morrison, J., Doeller, J. E., Kraus, D. W., Tao, L., Jiao, X., Scalia, R., Kiss, L., Szabo, C., Kimura, H., Chow, C. W., and Lefer, D. J. (2007) Hydrogen sulfide attenuates myocardial ischemia-reperfusion injury by preservation of mitochondrial function. *Proc. Natl. Acad. Sci. U.S.A.* **104,** 15560–15565
10. Sivarajah, A., McDonald, M. C., and Thiemermann, C. (2006) The production of hydrogen sulfide limits myocardial ischemia and reperfusion injury and contributes to the cardioprotective effects of preconditioning with endotoxin but not ischemia in the rat. *Shock* **26,** 154–161
11. Olson, K. R., and Whitfield, N. L. (2010) Hydrogen sulfide and oxygen sensing in the cardiovascular system. *Antioxid. Redox Signal* **12,** 1219–1234
12. Hosoki, R., Matsuki, N., and Kimura, H. (1997) The possible role of hydrogen sulfide as an endogenous smooth muscle relaxant in synergy with nitric oxide. *Biochem. Biophys. Res. Commun.* **237,** 527–531

13. Yang, G., Wu, L., Jiang, B., Yang, W., Qi, J., Cao, K., Meng, Q., Mustafa, A. K., Mu, W., Zhang, S., Snyder, S. H., and Wang, R. (2008) H_2S as a physiologic vasorelaxant. Hypertension in mice with deletion of cystathionine γ-lyase. *Science* **322,** 587–590
14. Wang, M. J., Cai, W. J., and Zhu, Y. C. (2010) Mechanisms of angiogenesis. Role of hydrogen sulfide. *Clin. Exp. Pharmacol. Physiol.* **37,** 764–771
15. Bhatia, M., Sidhapuriwala, J., Moochhala, S. M., and Moore, P. K. (2005) Hydrogen sulfide is a mediator of carrageenan-induced hindpaw oedema in the rat. *Br. J. Pharmacol.* **145,** 141–144
16. Collin, M., Anuar, F. B., Murch, O., Bhatia, M., Moore, P. K., and Thiemermann, C. (2005) Inhibition of endogenous hydrogen sulfide formation reduces the organ injury caused by endotoxemia. *Br. J. Pharmacol.* **146,** 498–505
17. Zhang, H., Zhi, L., Moochhala, S., Moore, P. K., and Bhatia, M. (2007) Hydrogen sulfide acts as an inflammatory mediator in cecal ligation and puncture-induced sepsis in mice by up-regulating the production of cytokines and chemokines via NF-kappaB. *Am. J. Physiol. Lung Cell. Mol. Physiol.* **292,** L960–L971
18. Cunha, T. M., Dal-Secco, D., Verri, W. A., Jr., Guerrero, A. T., Souza, G. R., Vieira, S. M., Lotufo, C. M., Neto, A. F., Ferreira, S. H., and Cunha, F. Q. (2008) A simultaneous plasma level and EEG assessment of an oral hypnotic (ethinamate). *Eur. J. Pharmacol.* **590,** 127–135
19. Zanardo, R. C., Brancaleone, V., Distrutti, E., Fiorucci, S., Cirino, G., and Wallace, J. L. (2006) Hydrogen sulfide is an endogenous modulator of leukocyte-mediated inflammation. *FASEB J.* **20,** 2118–2120
20. Li, L., Rossoni, G., Sparatore, A., Lee, L. C., Del Soldato, P., and Moore, P. K. (2007) Anti-inflammatory and gastrointestinal effects of a novel diclofenac derivative. *Free Radic. Biol. Med.* **42,** 706–719
21. Sivarajah, A., Collino, M., Yasin, M., Benetti, E., Gallicchio, M., Mazzon, E., Cuzzocrea, S., Fantozzi, R., and Thiemermann, C. (2009) Anti-apoptotic and anti-inflammatory effects of hydrogen sulfide in a rat model of regional myocardial I/R. *Shock* **31,** 267–274
22. Levine, J., Ellis, C. J., Furne, J. K., Springfield, J., and Levitt, M. D. (1998) Fecal hydrogen sulfide production in ulcerative colitis. *Am. J. Gastroenterol.* **93,** 83–87
23. Gibson, G. R., Cummings, J. H., and Macfarlane, G. T. (1991) Growth and activities of sulphate-reducing bacteria in gut contents of healthy subjects and patients with ulcerative colitis. *FEMS Microbiol. Lett.* **86,** 103–111
24. Pitcher, M. C., and Cummings, J. H. (1996) Hydrogen sulfide. A bacterial toxin in ulcerative colitis? *Gut* **39,** 1–4
25. Kanazawa, K., Konishi, F., Mitsuoka, T., Terada, A., Itoh, K., Narushima, S., Kumemura, M., and Kimura, H. (1996) Factors influencing the development of sigmoid colon cancer. Bacteriologic and biochemical studies. *Cancer* **77,** 1701–1706
26. Levitt, M. D., Furne, J., Springfield, J., Suarez, F., and DeMaster, E. (1999) Detoxification of hydrogen sulfide and methanethiol in the cecal mucosa. *J. Clin. Invest.* **104,** 1107–1114
27. Roediger, W. E., Moore, J., and Babidge, W. (1997) Colonic sulfide in pathogenesis and treatment of ulcerative colitis. *Dig. Dis. Sci.* **42,** 1571–1579
28. Brodie, A. E., Potter, J., and Reed, D. J. (1982) Unique characteristics of rat spleen lymphocyte, L1210 lymphoma, and HeLa cells in glutathione biosynthesis from sulfur-containing amino acids. *Eur. J. Biochem.* **123,** 159–164
29. Kamatani, N., and Carson, D. A. (1982) Differential cyst(e)ine requirements in human T and B lymphoblastoid cell lines. *Int. Arch. Allergy Appl. Immunol.* **68,** 84–89
30. Noelle, R. J., and Lawrence, D. A. (1980) Modulation of T cell functions. I. Effect of 2-mercaptoethanol and macrophages on T cell proliferation. *Cell. Immunol.* **50,** 416–431
31. Iwata, S., Hori, T., Sato, N., Ueda-Taniguchi, Y., Yamabe, T., Nakamura, H., Masutani, H., and Yodoi, J. (1994) Thiol-mediated redox regulation of lymphocyte proliferation. Possible involvement of adult T cell leukemia-derived factor and glutathione in transferrin receptor expression. *J. Immunol.* **152,** 5633–5642
32. Yan, Z., Garg, S. K., Kipnis, J., and Banerjee, R. (2009) Extracellular redox modulation by regulatory T cells. *Nat. Chem. Biol.* **5,** 721–723
33. Barathi, S., Vadhana, P., Angayarkanni, N., and Ramakrishnan, S. (2007) Estimation of hydrogen sulfide in the human lymphocytes. *Indian J. Biochem. Biophys.* **44,** 179–182
34. Mirandola, P., Gobbi, G., Sponzilli, I., Pambianco, M., Malinverno, C., Cacchioli, A., De Panfilis, G., and Vitale, M. (2007) Exogenous hydrogen sulfide induces functional inhibition and cell death of cytotoxic lymphocytes subsets. *J. Cell. Physiol.* **213,** 826–833
35. Li, L., Whiteman, M., Guan, Y. Y., Neo, K. L., Cheng, Y., Lee, S. W., Zhao, Y., Baskar, R., Tan, C. H., and Moore, P. K. (2008) Characterization of a novel, water-soluble hydrogen sulfide-releasing molecule (GYY4137): new insights into the biology of hydrogen sulfide. *Circulation* **117,** 2351–2360
36. Lee, Z. W., Zhou, J., Chen, C. S., Zhao, Y., Tan, C. H., Li, L., Moore, P. K., and Deng, L. W. (2011) The slow-releasing hydrogen sulfide donor, GYY4137, exhibits novel anti-cancer effects *in vitro* and *in vivo*. *PLoS One* **6,** e21077
37. Bunnell, S. C., Kapoor, V., Trible, R. P., Zhang, W., and Samelson, L. E. (2001) Dynamic actin polymerization drives T cell receptor-induced spreading. A role for the signal transduction adaptor LAT. *Immunity* **14,** 315–329
38. Tiranti, V., Viscomi, C., Hildebrandt, T., Di Meo, I., Mineri, R., Tiveron, C., Levitt, M. D., Prelle, A., Fagiolari, G., Rimoldi, M., and Zeviani, M. (2009) Loss of ETHE1, a mitochondrial dioxygenase, causes fatal sulfide toxicity in ethylmalonic encephalopathy. *Nat. Med.* **15,** 200–205
39. Atienza, J. M., Zhu, J., Wang, X., Xu, X., and Abassi, Y. (2005) Dynamic monitoring of cell adhesion and spreading on microelectronic sensor arrays. *J. Biomol. Screen* **10,** 795–805
40. Baratt, A., Arkhipov, S. N., and Maly, I. V. (2008) An experimental and computational study of effects of microtubule stabilization on T cell polarity. *PLoS One* **3,** e3861
41. Lowin-Kropf, B., Shapiro, V. S., and Weiss, A. (1998) Cytoskeletal polarization of T cells is regulated by an immunoreceptor tyrosine-based activation motif-dependent mechanism. *J. Cell Biol.* **140,** 861–871
42. de Kok, J. B., Roelofs, R. W., Giesendorf, B. A., Pennings, J. L., Waas, E. T., Feuth, T., Swinkels, D. W., and Span, P. N. (2005) Normalization of gene expression measurements in tumor tissues. Comparison of 13 endogenous control genes. *Lab. Invest.* **85,** 154–159
43. Smith, J. L., Collins, I., Chandramouli, G. V., Butscher, W. G., Zaitseva, E., Freebern, W. J., Haggerty, C. M., Doseeva, V., and Gardner, K. (2003) Targeting combinatorial transcriptional complex assembly at specific modules within the interleukin-2 promoter by the immunosuppressant SB203580. *J. Biol. Chem.* **278,** 41034–41046
44. Hara, T., Jung, L. K., Bjorndahl, J. M., and Fu, S. M. (1986) Human T cell activation. III. Rapid induction of a phosphorylated 28/32-kD disulfide-linked early activation antigen (EA1) by 12-*O*-tetradecanoyl phorbol-13-acetate, mitogens, and antigens. *J. Exp. Med.* **164,** 1988–2005
45. Vicente-Manzanares, M., and Sánchez-Madrid, F. (2004) Role of the cytoskeleton during leukocyte responses. *Nat. Rev. Immunol.* **4,** 110–122
46. Sechi, A. S., and Wehland, J. (2004) Interplay between TCR signaling and actin cytoskeleton dynamics. *Trends Immunol.* **25,** 257–265
47. Mustafa, A. K., Gadalla, M. M., Sen, N., Kim, S., Mu, W., Gazi, S. K., Barrow, R. K., Yang, G., Wang, R., and Snyder, S. H. (2009) H_2S signals through protein *S*-sulfhydration. *Sci. Signal.* **2,** ra72
48. Parsey, M. V., and Lewis, G. K. (1993) Actin polymerization and pseudopod reorganization accompany anti-CD3-induced growth arrest in Jurkat T cells. *J. Immunol.* **151,** 1881–1893
49. Cuthbert, J. A., and Shay, J. W. (1983) Microtubules and lymphocyte responses. Effect of colchicine and taxol on mitogen-induced human lymphocyte activation and proliferation. *J. Cell. Physiol.* **116,** 127–134
50. Valitutti, S., Dessing, M., Aktories, K., Gallati, H., and Lanzavecchia, A. (1995) Sustained signaling leading to T cell activation results from prolonged T cell receptor occupancy. Role of T cell actin cytoskeleton. *J. Exp. Med.* **181,** 577–584
51. Bucci, M., Papapetropoulos, A., Vellecco, V., Zhou, Z., Pyriochou, A., Roussos, C., Roviezzo, F., Brancaleone, V., and Cirino, G. (2010) Hydrogen sulfide is an endogenous inhibitor of phosphodiesterase activity. *Arterioscler. Thromb. Vasc. Biol.* **30,** 1998–2004
52. Papapetropoulos, A., Pyriochou, A., Altaany, Z., Yang, G., Marazioti, A., Zhou, Z., Jeschke, M. G., Branski, L. K., Herndon, D. N., Wang, R., and

Szabó, C. (2009) Hydrogen sulfide is an endogenous stimulator of angiogenesis. *Proc. Natl. Acad. Sci. U.S.A.* **106,** 21972–21977
53. Yong, R., and Searcy, D. G. (2001) Sulfide oxidation coupled to ATP synthesis in chicken liver mitochondria. *Comp. Biochem. Physiol. B Biochem. Mol. Biol.* **129,** 129–137
54. Griesbeck, C., Schütz, M., Schödl, T., Bathe, S., Nausch, L., Mederer, N., Vielreicher, M., and Hauska, G. (2002) Mechanism of sulfide-quinone reductase investigated using site-directed mutagenesis and sulfur analysis. *Biochemistry* **41,** 11552–11565
55. Gmünder, H., Eck, H. P., Benninghoff, B., Roth, S., and Dröge, W. (1990) Macrophages regulate intracellular glutathione levels of lymphocytes. Evidence for an immunoregulatory role of cysteine. *Cell. Immunol.* **129,** 32–46
56. Li, Z., He, L., Wilson, K., and Roberts, D. (2001) Thrombospondin-1 inhibits TCR-mediated T lymphocyte early activation. *J. Immunol.* **166,** 2427–2436
57. Garlie, N. K., LeFever, A. V., Siebenlist, R. E., Levine, B. L., June, C. H., and Lum, L. G. (1999) T cells coactivated with immobilized anti-CD3 and anti-CD28 as potential immunotherapy for cancer. *J. Immunother.* **22,** 336–345
58. Stern, J. B., and Smith, K. A. (1986) Interleukin-2 induction of T cell G_1 progression and c-myb expression. *Science* **233,** 203–206
59. Furne, J., Saeed, A., and Levitt, M. D. (2008) Whole tissue hydrogen sulfide concentrations are orders of magnitude lower than presently accepted values. *Am. J. Physiol. Regul. Integr. Comp. Physiol.* **295,** R1479–R1485
60. Jiang, B., Tang, G., Cao, K., Wu, L., and Wang, R. (2010) Molecular mechanism for H (2)S-induced activation of K (ATP) channels. *Antioxid. Redox Signal* **12,** 1167–1178
61. Telezhkin, V., Brazier, S. P., Cayzac, S. H., Wilkinson, W. J., Riccardi, D., and Kemp, P. J. (2010) Mechanism of inhibition by hydrogen sulfide of native and recombinant BKCa channels. *Respir. Physiol. Neurobiol.* **172,** 169–178
62. Yong, Q. C., Lee, S. W., Foo, C. S., Neo, K. L., Chen, X., and Bian, J. S. (2008) Endogenous hydrogen sulfide mediates the cardioprotection induced by ischemic postconditioning. *Am. J. Physiol. Heart Circ. Physiol.* **295,** H1330–H1340
63. Zhu, X. Y., Liu, S. J., Liu, Y. J., Wang, S., and Ni, X. (2010) Glucocorticoids suppress cystathionine γ-lyase expression and H_2S production in lipopolysaccharide-treated macrophages. *Cell. Mol. Life Sci.* **67,** 1119–1132
64. Garg, S. K., Yan, Z., Vitvitsky, V., and Banerjee, R. (2011) Differential dependence on cysteine from transsulfuration *versus* transport during T cell activation. *Antioxid. Redox Signal* **15,** 39–47
65. Wilson, K., Mudra, M., Furne, J., and Levitt, M. (2008) Differentiation of the roles of sulfide oxidase and rhodanese in the detoxification of sulfide by the colonic mucosa. *Dig. Dis. Sci.* **53,** 277–283
66. Taniguchi, E., Matsunami, M., Kimura, T., Yonezawa, D., Ishiki, T., Sekiguchi, F., Nishikawa, H., Maeda, Y., Ishikura, H., and Kawabata, A. (2009) Rhodanese, but not cystathionine-γ-lyase, is associated with dextran sulfate sodium-evoked colitis in mice. A sign of impaired colonic sulfide detoxification? *Toxicology* **264,** 96–103
67. Medani, M., Collins, D., Docherty, N. G., Baird, A. W., O'Connell, P. R., and Winter, D. C. (2010) Emerging role of hydrogen sulfide in colonic physiology and pathophysiology. *Inflamm. Bowel Dis.* **17,** 1620–1625